

WiFi-ID: Human Identification using WiFi signal

Jin Zhang^{*†}, Bo Wei[‡], Wen Hu^{*†}, Salil S. Kanhere^{*}

^{*}School of Computer Science and Engineering, The University of New South Wales, Australia
Email: {jin.zhang1, wen.hu, salil.kanhere}@unsw.edu.au

[†]CSIRO Digital Productivity Flagship, Australia

[‡]Department of Computer Science, University of Oxford, UK Email: {bo.wei}@cs.ox.ac.uk

Abstract—Prior research has shown the potential of device-free WiFi sensing for human activity recognition. In this paper, we show for the first time WiFi signals can also be used to uniquely identify people. There is strong evidence that suggests that all humans have a unique gait. An individual’s gait will thus create unique perturbations in the WiFi spectrum. We propose a system called WiFi-ID that analyses the channel state information to extract unique features that are representative of the walking style of that individual and thus allow us to uniquely identify that person. We implement WiFi-ID on commercial off-the-shelf devices. We conduct extensive experiments to demonstrate that our system can uniquely identify people with average accuracy of 93% to 77% from a group of 2 to 6 people, respectively. We envisage that this technology can find many applications in small office or smart home settings.

I. INTRODUCTION

Wireless devices are everywhere - our homes, offices, shops, restaurants and virtually all of our urban spaces. They invisibly fill the air with a spectrum of Radio Frequency (RF) signals. When a person walks through these spaces, they create a perturbation in this RF field. By closely examining these perturbations using the Channel State Information (CSI), it is possible to identify basic human activities such as standing, sitting, walking and running [25] and even hand gestures [19] and keystrokes typed on a keyboard [3].

In this paper, we show for the first time that WiFi signals can also be used to uniquely identify people. Everyone’s natural walking style (i.e. gait) is unique which is characterized by the differences in the limb (hand and feet) movement patterns and velocity [15]. These patterns are also highly repetitive. Our hypothesis is that an individual’s gait will thus create a unique perturbation in the WiFi spectrum. Fig. 1 shows the spectrogram of the CSI data for two people walking through the same corridor (scenario depicted at the top of Fig. 1). One can readily observe the differences manifested by each person’s unique gait; particularly in the segment of the data where the subjects cross the Line of Sight (LoS) path between the two wireless devices. Prior research has demonstrated that unique gait signatures can be extracted from video sequences that capture people walking [22] and from an array of a large number of pressure-sensitive sensors deployed underneath a floor for measuring foot pressure patterns [6] [17].

Our work is different, since we rely on passive reception of WiFi signals from infrastructure which is already ubiquitous in our surroundings. The device-free and non-intrusive nature

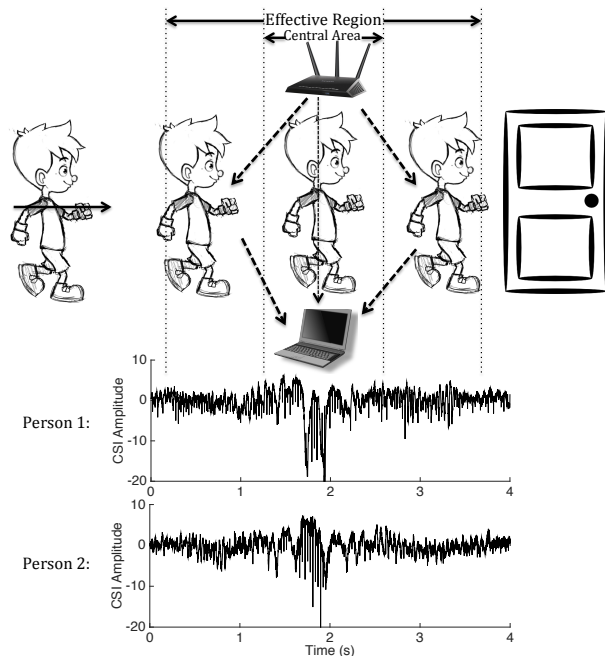


Fig. 1. Operational Scenario for WiFi-ID

of this approach makes it an attractive alternative to traditional authentication methods that use cameras, microphones, biometrics or physical objects (swipe cards, wearable tags, etc). Camera systems [23] require line of sight and sufficient ambient light. Audio and visual approaches also give rise to significant privacy concerns. Wearable sensors [12] [11] rely on the unique signatures generated by embedded Inertial Measurement Unit (IMU) sensors but often are required to be worn in a specific manner to ensure accurate operations. Biometric sensors such as fingerprints are susceptible to hacking. In contrast, our radio based approach is less intrusive and uses existing WiFi infrastructure, and thus has broad applications for authenticating individuals in smart homes, offices and assisted living facilities.

The general problem of uniquely identifying an individual from a large user population in any physical setting is arguably very challenging. To make the problem more tractable, we consider a setting where the goal is to uniquely identify a person from a group of N people. This is representative of a smart home or small office setting. Consider for example a smart home where children may be prohibited access by themselves into the garage or home office. Or a smart office where only selected staff have access to certain offices (e.g., server room

or file storage). Moreover, we consider a simple yet common scenario for a home or office setting, wherein a single person (from a group of N people) walks through a corridor towards a door as depicted. The goal is to uniquely identify this person so as to either permit or deny access to the room behind the door.

In this paper, we propose WiFi-ID, a WiFi based human identification system that is deployed on commercial off-the-shelf WiFi devices. A transmitter node (any typical WiFi AP) continuously sends packets to a receiver node (e.g. laptop) which passively records CSI data from the received packets. The CSI data captures the aggregate impact of multi-path, shadowing and interference on the WiFi signals in a given environment. When a person walks, their gait impacts the environment in a unique manner, which changes the effect of these phenomena on the WiFi signal. It is expected that these are in turn manifested as unique perturbations in the CSI data. There are several challenges in realising human identification, even in this seemingly simplified setting.

The CSI time series constitutes data from multiple transmit (N_t) and receive (N_r) antenna pairs each comprised of multiple subcarriers (e.g., 30 OFDM subcarriers for 802.11n). The first technical challenge is to determine if the CSI data is rich enough to capture unique signatures of a person's gait. Prior work [24] has suggested that the perturbations caused by the motion of human limbs (hand and feet) while walking is typically concentrated in certain specific RF bands. Using empirical measurements we demonstrate that the effects of human gait are most pronounced in the 20-80 Hz frequency bands for 5GHz WiFi. We adopt the FFT based Continuous Wavelet Transformation (CWT) method for extracting the signals in the different frequency bands.

The second challenge is to find distinguishing features that can be used to uniquely identify an individual. In order to find the unique patterns of each person we compute multiple features from the CSI data. These features preserve both time and frequency domain information of the CSI time series in order to capture the effects of the gait patterns on an individual. However, given the dimension of the CSI data, the resulting feature set is very large. We apply ReliefF, an efficient feature selection algorithm to rank the various features.

The third challenge is to segment the CSI time series data to extract the part of the signal which has the most pronounced effect due to the motion of the person, i.e. which corresponds to the effective region in Figure 1. We design a silence removal method which analyse the short time energy of the CSI time series data to determine the start and end points of the effective region.

We conduct extensive experiments to evaluate performance of WiFi-ID using 20 subjects in a scenario consistent with Figure 1. Our system can uniquely identify a person with an average accuracy from 93% to 77% from a group size of 2-6 people, respectively.

The remaining paper is organised as follows. Section II discuss the related work and introduce CSI in details in Section III. Section V shows the silence removal for movement

extractions. The signal separation is described in Section VI. Section VII introduces the feature extractions and hybrid feature selection approach. Section VIII shows SAC classification. Section IX shows the implementation and comprehensively evaluate the system. Section X concludes the paper.

II. RELATED WORK

Human identification has been researched for a decade. [23] and [22] all use video cameras to record people walking and extract patterns from images. [23] and [22] both capture the silhouette of persons and extract the gait motions of persons for identifications. While the above camera-based approaches achieve good accuracy in identifying individual's they could be considered to be too intrusive (from the perspective of privacy) for use in offices and homes. Moreover, their results are dependent on good lighting conditions. Other works exploit fingerprints [2], iris [13] or sclera [30] biometrics for identifications. The accuracy of these approaches is higher than using video cameras. However collecting biometric data often makes users uncomfortable and limit their applications. Moreover, several researchers have demonstrated that such biometric systems can be faked [1]. [12] and [11] use wearable sensors and derive signatures that are unique to an individual's activity, which in turn can be used to identify people. However, these methods require that the sensors must be worn in a specific manner to ensure accurate operations. Moreover, not everyone is comfortable wearing such sensors on their body at all times. Our work is different in that it leverages the existing WiFi infrastructures for human identifications without the need for additional sensors and intrusive monitoring.

Recently many works use wireless radio for human body sensing. [16] considers the micro Doppler detected by radars for human gait recognitions. However the utilisation of radars is limited due to high costs and regulations. [25], [29] and [24] utilise channel state information (CSI) reported from WiFi cards for human activity recognition. Unlike RSSI which provides the coarse information about the received signal strength, CSI data contain rich information from every wireless sub-channels. Various human activities such as sitting, walking and running create unique perturbations in the CSI data and can thus be used to recognise these activities [25]. In [29], the authors propose a CSI-speed model that establishes a relationship between the CSI variations and the speed of human movement. CSI data has also be used to recognise hand gestures [19] and keystrokes [3] typed on a keyboard. Our work is a natural evolution of this prior work. We show for the first time that CSI data can be used to uniquely identify individuals.

III. CHANNEL STATE INFORMATION

In this section, we provide a short overview of Channel State Information (CSI). Most modern off-the-shelf WiFi devices support the IEEE 802.11n/ac standard and typically include multiple antennas for MIMO communications. These devices operate on both the 2.4GHz and 5 GHz bands and employ OFDM at the PHY layer. The WiFi NICs continuously monitor

the frequency response of OFDM subcarriers as Channel State Information (CSI) [28]. Unlike RSSI that represent the total received signal strength at the receiver, CSI contains information of individual subcarriers between each pair of transmit and receive antenna. Therefore the CSI can capture the effects of multiple wireless phenomena such as frequency selective fading, shadowing, multipath, destructive and constructive interference. The CSI information is very useful and can be used for improving the link quality of WiFi connections.

Let N_t and N_r represent the number of transmit and receive antennas. Thus the MIMO system constitute $N_t \times N_r$ antenna pairs. Let Y_i^p and X_i^p represent the frequency response for subcarrier i and antenna pair p . Let H_i^p denote the Channel Frequency Response (CFR) at any time instant. Then,

$$Y_i^p = H_i^p \times X_i^p \quad i \in [1, C] \quad p \in [1, N_t \times N_r] \quad (1)$$

H_i^p is a complex value and $\|H_i^p\|$ simplified as h_i^p denote its amplitude. In this work we focus on amplitude. In our future work, we plan to explore phase information. The time series of h_i^p are called CSI streams. The customised driver of the Intel 5300 NIC [5] which is used in our experiments reports 30 OFDM subcarriers of 802.11n between each antenna pair (i.e. $C = 30$). Thus the total dimension of the CSI time series is $30 \times N_t \times N_r$.

IV. OVERVIEW OF WiFi-ID

We consider the scenario depicted in Fig. 1 as the operational setting for our system. Our system, WiFi-ID consists of a transmitter (typically an AP) which periodically transmits (or are these broadcast) packets which are captured by a receiver which is capable of extracting the CSI information as discussed in Section III. Our system has two operational phases - training and testing. In each phase we ask the same set of individuals to walk normally along the corridor (depicted in Section III) in a straight line by themselves. The CSI data collected during the training phase is used to identify features that are unique to each individuals' gait, which in turn are stored in a database. The CSI data collected during the testing phase are processed in a similar manner to extract the same set of features which are then matched with those in the database to uniquely identify the test subjects.

Fig. 2 depicts the basic building blocks of WiFi-ID. In the first step, WiFi-ID segments the CSI time series data to extract the portion of the signal which corresponds to the effective region depicted in Section III. This portion of the signal has the most pronounced impact of the human gait and is thus most interesting to analyze. We employ a silence removal algorithm that uses the short time energy of the CSI signal for this purpose (see Section V). As will be explained in Section VI, we analyzed the CSI data to determine if the influence of the human gait is particularly pronounced in specific frequency bands. Our investigation revealed that the CSI data in the 20 - 80 Hz frequency band for 5GHz WiFi contained the most unique features that are representative of the individual's gait (see Section IX). Hence, WiFi-ID employs a signal separation module (see Section VI) that

uses Continuous Wavelet Transformation (CWT) to extract signals in different frequency bands. Next, WiFi-ID uses the RelieF feature selection algorithm to compute various time and frequency domain features from the CSI data in the selected frequency bands (see Section VII). We use a subset of the feature set to represent the fingerprint of each individual. Finally, WiFi-ID uses Sparse Approximation based Classification (SAC) to determine the identity of the subject (see Section VIII).

V. SILENCE REMOVAL AND SEGMENTATION

Note that, the transmitter and receiver in WiFi-ID are operating continuously, i.e. the transmitter repeatedly sends packets and the receiver extracts the CSI data from the received packets. In the absence of people moving along the corridor, the CSI data will capture the effect of the ambient noise from other RF transmissions in the vicinity. This data is not useful and must be discarded. On the contrary, when a person walks along the corridor, the corresponding CSI data is used for identifying the individual. In particular, we are interested in the CSI data that corresponds with the motion of the person in the *effective region* depicted in Fig. 1, since this where their motion would have the most pronounced impact on the WiFi spectrum. There are two key challenges here. The first challenge is determining the length (or duration in terms of time) of this effective region. If the region is set to be too short, then the corresponding CSI stream may not capture sufficient information that is representative of a person's gait. On the other hand, if the region is too large, then the CSI stream will also include parts of the signal which are not impacted by the human motion. We use the parameter T to represent the duration of the effective region. In Section IX we comprehensively evaluate the impact of varying the duration of T .

The second challenge is to determine the start point of the effective region. An error in determining this will result in the exclusion of some part of the useful signal that contains representative information and instead include parts of the CSI stream that are not as meaningful. Observe from Fig. 1, that the CSI data does not exhibit abrupt changes as a person enters the effective region. Hence, a simple thresholding approach is unlikely to work. Moreover, such a threshold may not be uniformly applicable to all people as each person may impact the CSI data in a unique manner. In addition, such a threshold may not be robust to changing environmental conditions.

In the following, we outline our approach to addressing these two challenges. Observe from Fig. 1 that when the person is directly crossing the LoS path between the transmitter and receiver, the impact of their motion is most pronounced on the CSI data. We refer to this part of the effective region as the central area. In our silence removal approach (outlined in Algorithm 1), we aim to identify the approximate mid point of this central area and then back track and determine the start point of the effective region. As discussed in Section III, the CSI data consists of $30 \times N_t \times N_r$ streams all of which exhibit similar perturbations due to the human motion. We

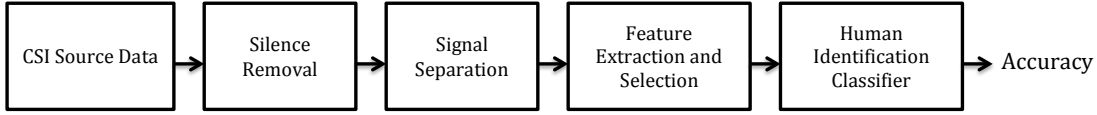


Fig. 2. Overview of the WiFi-ID system.

select one arbitrary stream h_i^p . A Butterworth filter is applied on h_i^p to remove the high frequency noise. Next, we partition the stream into short frames S_j of duration 0.05 seconds and calculate the short time energy E_j for each frame. A median filter and log calculation are used to smooth the vector \mathbf{E} , which represents the short time energy of all frames S . The average value of \mathbf{E} is determined and used as a threshold to identify the central region. Precisely, a contiguous block of frames S_{mid} , for which the energy of each frame is above the threshold is chosen. The portion of the original signal h_i^p that corresponds to the frames S_{mid} is selected to be the central region, h_{mid} . Next we determine the mid-point of this region, m , as the instantaneous signal which has the maximum deviation from the average in h_{mid} . Since the duration of the effective region is T , the start point can be located at $m - T/2$. The selected CSI data of duration T , \mathcal{H} , represents the dataset from one walking experiment.

Algorithm 1 Silence Removal

- 1: **Input:** An arbitrary CSI stream h_i^p filtered by butterworth and duration T
 - 2: partitioned into a sequence of frames $S_j(n)$, $j \in [1, Z]$, $n \in [1, N]$, where Z is the total number of frames, each frame has N CSI values
 - 3: **for** each frame $j = 1 : Z$ **do**
 - 4:
$$E_j = \frac{1}{N} \sum_{n=1}^N |S_j(n)|^2$$
 - 5: **end for**
 - 6: $E = \log(\text{MedianFilter}(E))$
 - 7: select S_{mid} which $E_j > \text{mean}(E)$ and map to h_{mid}
 - 8: calculate the mid point m with maximum deviations and the Start Point is $m - T/2$ in h_i^p
 - 9: apply Start Point to other CSI streams h
 - 10: **Output:** One walk observation dataset \mathcal{H}
-

VI. SIGNAL SEPARATION

The output of the silence removal, \mathbf{H} , corresponds to the CSI data consisting of $30 \times N_t \times N_r$ time streams that captures the impact of a person walking through the effective region. In this section, we analyze \mathbf{H} to understand how a person's gait uniquely impacts the CSI signal. This will offer insights on how we can find distinguishing features that allow us to uniquely identify an individual. To observe the signal energy in different frequency bands as a function of time, we plot the spectrogram for walk observations from two different people in Fig. 3. It is evident that the spectrograms have some similarities and differences at the same time. Both observations exhibit strong energy in the low frequency bands (<30Hz) and lower energy in higher frequency bands (>100Hz). At the

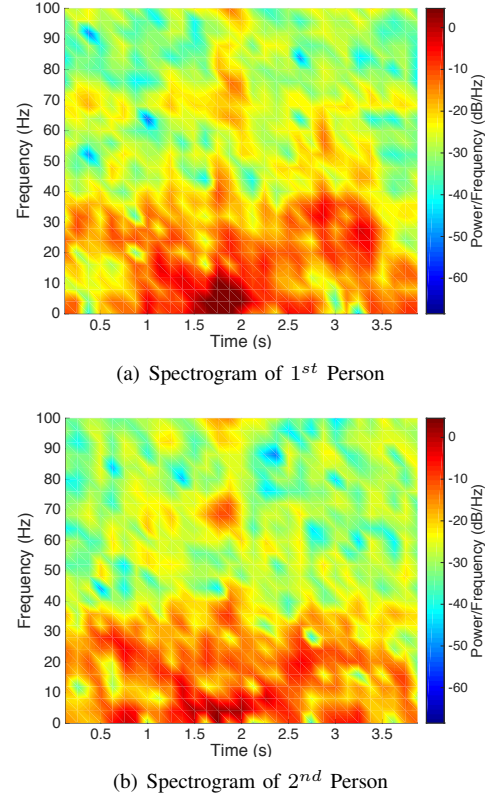


Fig. 3. Comparison between spectrograms of two persons.

same time, the first spectrogram appears to have more energy (i.e. more red regions) across all frequency bands compared to the second. This initial investigation suggests that there may be some merit to analyze the CSI data in different frequency bands.

The authors in [24] conducted experiments in a similar setting as ours (i.e. Fig. 1) and demonstrated that there is a correlation between the velocity of movement of human limbs and the frequency components of the CSI stream where the impact of this motion is most pronounced. Specifically the frequency is equal to the velocity of the motion divided by WiFi carrier wavelength. Prior work [21] has also shown that different parts of the human body exhibit different velocities. For example, the average velocity of human limbs (hands and legs) is around 2m/s whereas the human torso moves at approximately 1m/s. This suggest that the impact of a person's gait is likely to be most pronounced in a specific frequency band of the CSI data, specifically the band that maps to velocities in the range of 1m/s to 2m/s. WiFi-ID uses the 5.18 GHz band which has a wavelength of 5.79cm. The corresponding frequency band 20Hz - 80Hz is thus worth analyzing further. The above also suggests that higher frequencies are unlikely contain any meaningful information

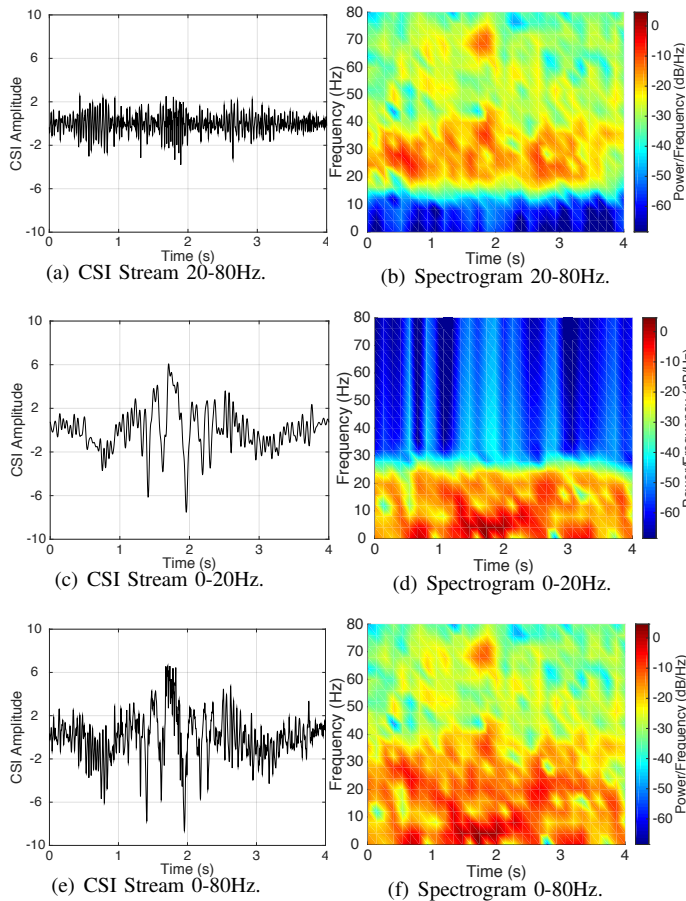


Fig. 4. The three frequency bands of interest. (a)(c)(e) illustrate the CSI stream and (b)(d)(f) show the spectrograms.

representative of human motion. This is also evident from the spectrograms in Fig. 3. Hence, we exclude the frequencies above 80Hz.

Prior work [4] has shown that the human body can be modelled as a conducting cylinder when studying its impact on the WiFi spectrum. When a person walks across the central area (in Fig. 1) and crosses the direct LoS between the transmitter and receiver, the WiFi spectrum is influenced by a mixture of multipath and shadowing effects. This is manifested by the strong energy observed in the lower frequency bands (<20Hz) as observed in Fig. 3. Thus, the low frequency band of 0-20Hz is also worth investigating further.

In summary, we consider two specific frequency bands for further investigation - (i) 20-80Hz and (ii) 0-20 Hz in order to determine which part of the signal is most likely to exhibit distinguishing features specific to an individual's gait. We also include the combined 0-80Hz frequency band as a baseline.

In order to separate these signals WiFi-ID use FFT based Continuous Wavelet Transformation (CWT) [20] and Morlet wavelet [7] to transform CSI streams into wavelet domain. WiFi-ID then applies Inverse CWT to restore the selected signal in particular frequency bands. Compared with Short Time Fourier Transform(STFT) [26], CWT is more effective in restoring highly varying signals such as impulse and peaks.

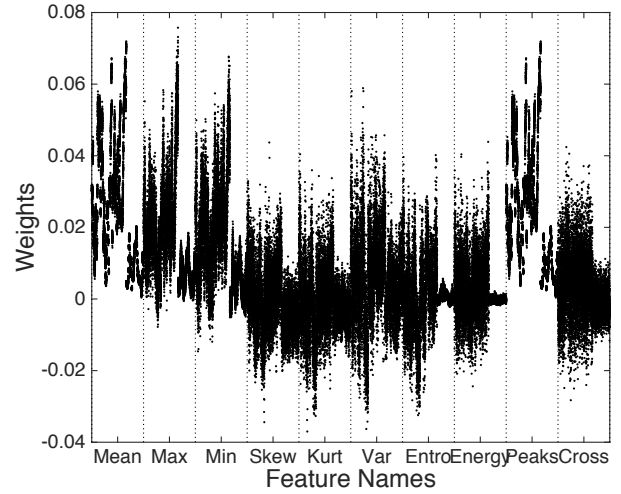


Fig. 5. Weights of all feature attributes

WiFi-ID chooses 6-9, 10-23 and 6-23 wavelet scales combinations for the signals in 20-80Hz, 0-20Hz and 0-80Hz frequency bands respectively [10].

Fig. 4 illustrates the three separated signals and their corresponding spectrograms. Observe that the 20-80Hz signal in Fig. 4(a) has little similarity with the 0-80Hz signal in Fig. 4(e). In contrast the 0-20Hz signal has a similar envelop as the 0-80Hz signal. As will be elaborated in Section IX, we observe that the 20-80Hz signal has the most unique features which are useful for identifying an individual. Hence, WiFi-ID uses this particular frequency band during its operation. In the next section, we outline our feature selection procedure.

VII. FEATURE EXTRACTION AND SELECTION

Our goal herein is to analyze the 3 datasets discussed in Section VI and identify the features that are most representative of the individual's gait and thus help in achieving high accuracy in uniquely identifying people. In this section we outline how WiFi-ID accomplishes feature extraction and selection.

Recall that the CSI stream consists of $30 \times N_t \times N_r$ subcarriers. Prior work on classifying human activities from CSI data [8] [9] have shown that a part of the subcarriers contain sufficient information for activity detection. As will be shown later in this section, this does not hold true for our purposes. Hence we use the comprehensive data from all subcarriers. We segment the CSI time series data in each stream using a window size of 0.1 seconds. For each window we compute a comprehensive set of statistical features. Specifically WiFi-ID makes use of 7 time domain features - mean, max, min, skewness, kurtosis, variance and mean crossing rate and 3 frequency domain features - normalized entropy, normalized energy and the largest FFT peaks. The time domain features are able to measure the patterns of the CSI waveform, while the frequency domain features analyse the energy distribution information. Similar features have been used in prior work on human activity recognition using CSI data [29]. and motion sensors such as accelerometer [14].

The above 10 features are computed for each CSI stream resulting in a very large feature space of dimension - $10 \times$

$30 \times N_t \times N_r \times T/0.1$. For example, if $T = 4$ seconds, then we have 108000 feature attributes. Using the entire feature set for classification is obviously very time consuming. Moreover, not all features may be useful for classification purposes and may thus introduce noise. Hence, we employ feature selection to identify the most useful features that are pertinent for uniquely identifying an individual. We adopt ReliefF, an efficient feature selection algorithm [18]. ReliefF is a filter-based feature selection method with a low-order polynomial time complexity. In our context, ReliefF estimates the qualities of feature attributes, represented by a weight, based on how well they distinguish multiple individuals. The feature attributes with high weights are selected and used for classification.

Fig. 5 shows the feature weights from the 20-80 Hz dataset of one individual. The y-axis represents the weights while the x-axis represents the feature categories. Each category consists of $30 \times N_t \times N_r \times T/t$ points, corresponding to the total number of streams. We observe that the FFT peaks and mean generally have higher weights than the other features. Moreover, the time domain features tend to have higher weights than the frequency domain features. It is also evident from Fig. 5 that different sub-carriers have high weights across different feature categories. This confirms that the impact of the gait is manifested in varying degree by all sub-carriers. This lends credence to our earlier argument a subset of carriers are not sufficient for identifying distinct features. Next, we rank the weights of all attributes in descending order and select the top R percentage of features. In Section IX we comprehensively evaluate the impact of R on the detection accuracy.

VIII. CLASSIFICATION

In this section we outline the classification algorithm employed in WiFi-ID. In [27], Wright et.al. proposed Sparse Approximation based Classification (SAC) for face recognition and showed that it is robust to noisy features due to the usage of ℓ_1 minimisation. Even though WiFi-ID employs feature selection to find representative features, it was shown in Fig.5 that generally all features have low weights, which suggests that they may include some ineffective information. Hence, we chose to use SAC as the classifier.

To model human identification as a sparse representation problem, we first build a dictionary containing the features selected in the previous section. Consider the scenario where we wish to identify a person that belongs to a group of n people. Assume that we have l walking observations per person as training samples which collected in training phase of the system. Each walking observation is a p dimensional feature vector which are the R percentage features discussed in the previous section. We assemble the feature vectors of i -th person in a $p \times l$ sub-dictionary F_i . The feature datasets of n people can be compiled to form a $p \times ln$ dictionary $F = [F_1, \dots, F_i, \dots, F_n]$ $i \in [1, n]$. Let β denotes a test sample (i.e. a new walk observation) from one of the people from this group. It can be represented by the following linear equation $\beta = F\alpha$, where α is an unknown coefficient vector. If β belongs to the

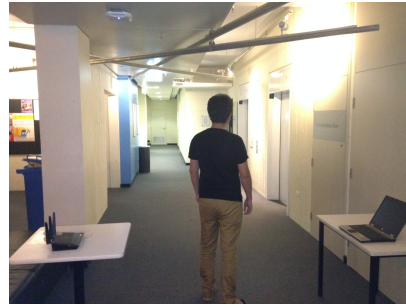


Fig. 6. A corridor where experiments conducted.

i -th person, β can be expressed by the linear combination of l feature vectors in F_i , and independent of the other $n - 1$ persons. So $\alpha = [0, \dots, 0, \alpha_{k,1}, \alpha_{k,2}, \dots, \alpha_{k,l_k}, 0, \dots, 0]^T$, the non-zeros entries of α that are related to the i -th person encode the identity of the test sample. However, due to the presence of noise, it is difficult to estimate α . In order to obtain α , ℓ_1 optimisation is used by SAC:

$$\hat{\alpha} = \arg \min_{\alpha} \|\alpha\|_1 \quad \text{subject to } \|\beta - F\alpha\|_2 < \epsilon, \quad (2)$$

where ϵ denote the noise value. After obtained $\hat{\alpha}$ from ℓ_1 optimisation, we can determine identity of the test sample by setting the coefficients of the other classes to zeros and calculating residuals, which is $r_i = \|\beta - F\hat{\alpha}_i\|_2$. The i -th person with the minimum residual will be the classification result (i.e. the identified person) of the test sample.

IX. EVALUATION

In this section we present a comprehensive evaluation of the WiFi-ID system. Section IX-A outlines the experimental setup. Section IX-B compares the different frequency bands outlined in Section VI to determine which part of the signal contains the features that are most representative of the individuals' gait. In Section IX-C we study the impact of varying the percentage of features, R and the duration of the effective region T on the classification accuracy. Finally, Section IX-D evaluates the classification accuracy of WiFi-ID for varying group sizes.

A. Experiment Setup

We implemented a prototype of WiFi-ID using off-the-shelf devices. The prototype consists of two devices: one HP 8530p laptop equipped with an Intel WiFi link 5300 802.11n chipset which acts as the receiver and one WiFi access point (AP) Netgear R7000 which serves as the transmitter. We installed Ubuntu 10.10 with modified Intel NIC driver [5] in the HP laptop. Both the transmitter and receiver have 3 antennas (i.e. $N_t = 3$ and $N_r = 3$). This gives us 30 (sub-carriers) $\times 3 \times 3 = 270$ data streams. Section IX illustrates the corridor scenario used in our experiments. The two devices were approximately 2 meters apart and placed on tables at a height of 1 meters. The entire WiFi-ID system depicted in Fig. 1 was implemented on the laptop in MATLAB.

We use the 5.19 GHz frequency band for all our experiments. The CSI data is recorded at a sampling rate of 800 Hz since we observed that using a lower sampling rate led to unstable measurements of the CSI data. The CSI data recorded

TABLE I
COMPARISON OF THE SIGNALS IN THREE DIFFERENT FREQUENCY BANDS.

	Accuracy (%)	Standard Deviation
H1 20-80 Hz	72.70	8.64
H2 0-20 Hz	60.80	16.25
H3 0-80 Hz	54.90	16.31

at the receiver is processed in MATLAB. The experiments were conducted in the corridor depicted in Section IX in our building. The campus WiFi network was operational the entire time. On occasion other building occupants passed by the vicinity but did not directly interfere with our experiments. We conducted two sets of experiments - the first with 10 subjects and the second with 20 subjects. Subjects were both male and female and aged between 25 to 28 years. The subjects were asked to walk in both directions through the corridor. Each subject was asked to walk 10 times thus resulting in 20 walking observations. The data collected from the first set of experiments was used to feature selection and model fine-tuning. The data from the second set of experiments was used for performance evaluation. We employed standard 10-fold cross validation to evaluate the accuracy. We used two evaluation metrics - (i) true detection rate (accuracy) and (ii) confusion matrix.

B. Comparing Different Frequency Bands

As discussed in Section VI, we wish to examine which of the following frequency bands contains features that are most representative of the individuals' motion: (i) 20-80 Hz (ii) 0-20 Hz and (iii) 0 to 80 Hz. We randomly select data from 5 subjects and produce the CSI data streams corresponding to these three frequency bands. The experiment are repeated for 20 times. For this set of evaluations we use all features (i.e. R from Section VII is equal to 100%). Table I shows the classification accuracy for the 3 datasets. The 20-80 Hz data clearly achieves better accuracy. This suggests that the signal in the 20 to 80Hz frequency band contains the most informative features for people classification. Hence, we only use data in this frequency band in the rest of the evaluations.

C. Effect of the duration of the effective region T and the fraction of features R

Recall that T denotes the duration of the effective region (Section V) and R represents the top- R % of the feature space (ordered in decreasing order of weights) that are used for classification (Section VIII). Herein, we study the impact of both these parameters on the classification accuracy. We use CSI data from five randomly chosen subjects in the 20-80 Hz frequency band for these experiments. We vary R from 1% to 90% (in increments of 10) and vary T from 1sec to 4 sec. The experiments are repeated 20 times and we report the mean accuracy and 95% confidence intervals in Fig. 7. We observe that the best performance is achieved when R is between 20% to 40%. and T is 4 seconds. Hence, we use $R = 40\%$ and $T = 4$ seconds in the rest of the evaluations.

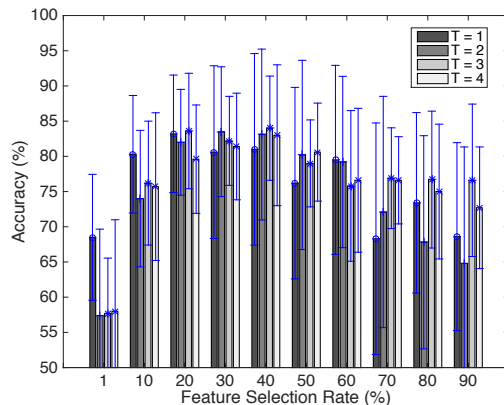


Fig. 7. Impact of feature selection rate and duration of effective region

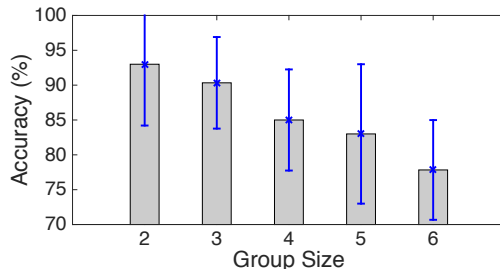


Fig. 8. Impact of group size

D. Effect of group sizes

In this sub-section we evaluate the performance of WiFi-ID considering a scenario where we wish to identify an individual that belongs to a group of N people. This is typical of a small office or home setting. Note that, we do not consider a scenario where a potential intruder (who does not belong the group) is trying to gain access. In this setting the intruder should not be misclassified as a group member. We leave this for future work. We vary N from 2 to 6. Recall that we have collected data from 20 subjects in our experiments. For each value of N we randomly select 20 combinations of groups of N people from the pool of 20 subjects. As expected, Fig. 8 shows that the accuracy decreases with an increase in group size. However, this result is consistent with other biometric authentication schemes such as face recognition. Nevertheless, the average accuracy is well over 80% for all group prizes.

Fig. 9 showed the confusion matrices for four different group sizes. Here, we randomly selected a number of (3, 4, 5, 6 respectively) subjects, and repeated experiments with the same group of people because we need to have the same group members to produce meaningful results. Therefore, the results in Fig. 9 could be seen as a subset of those reported in Fig. 8. We have also produced the confusion matrices with different group members and found similar results. Fig. 9 shows that most individuals can be identified uniquely in a group with high probability.

X. CONCLUSION

In this paper we present WiFi-ID a WiFi-based device-free human identification system. Each individual has a unique walking style and body shape. These in turn create unique

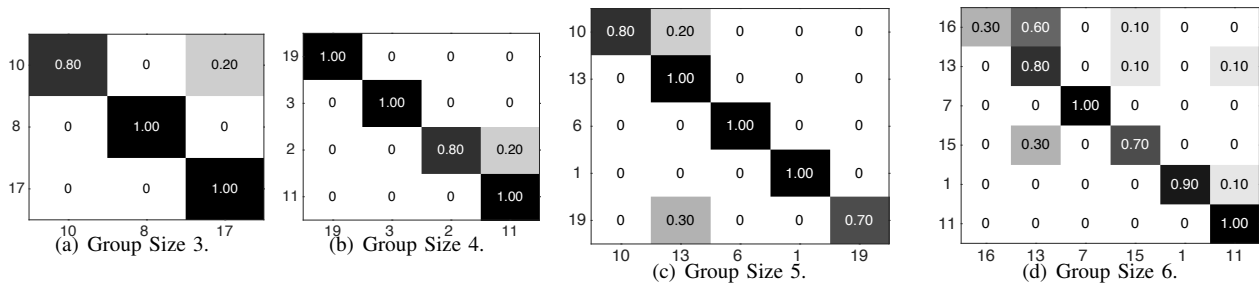


Fig. 9. Confusion matrices of four group sizes (3, 4, 5, 6). They x and y axis indicate the index of the participants.

perturbations when the person walks through the WiFi spectrum. WiFi-ID analyses these perturbations observed in the CSI data to identify unique features that allow identification of individuals. WiFi-ID achieved 93% to 77% human identification accuracy for 2 to 6 individuals in a group, respectively. We anticipate that WiFi-ID could be used in a small office setting or a smart home for personalised interaction with smart devices.

While our preliminary results are promising, we also acknowledge several limitations which need to be addressed to develop a more generalised solution. First, we have considered a simple (though practical) scenario wherein the participants directly cut across the Line of Sight (LoS) path between the transmitter and receiver. In the future we plan to conduct additional experiments in other settings such in a home or office and also consider non-LoS scenarios. Second, in our experiments we have only considered a simple setting of identifying a person from a maximum group size of 6 people. In our future work, we plan to consider larger group sizes and also robustness to false identification, i.e. incorrectly identifying a person who does not belong to the original group to be a part of it.

REFERENCES

- [1] Hack apple touch id. <http://www.theverge.com/2013/9/22/4759128/chaos-computer-club-biometric-hack-apple-touch-id>. Accessed: 2016-02-05.
- [2] P. Airey and J. Verran. A method for monitoring substratum hygiene using a complex soil: The human fingerprint. *Fouling, cleaning and disinfection in food processing*, 2006.
- [3] K. Ali et al. Keystroke recognition using wifi signals. In *Proceedings of the 21st Annual International Conference on Mobile Computing and Networking*, pages 90–102. ACM, 2015.
- [4] M. Ghaddar et al. A conducting cylinder for modeling human body presence in indoor propagation channel. *IEEE Transactions on Antennas and Propagation*, 55(11):3099–3103, 2007.
- [5] D. Halperin et al. Tool release: Gathering 802.11 n traces with channel state information. *ACM SIGCOMM Computer Communication Review*, 41(1):53–53, 2011.
- [6] A. Kale et al. Gait analysis for human identification. In *Audio-and Video-Based Biometric Person Authentication*, pages 1058–1058. Springer, 2003.
- [7] J. Lin and L. Qu. Feature extraction based on morlet wavelet and its application for mechanical fault diagnosis. *Journal of sound and vibration*, 234(1):135–148, 2000.
- [8] J. Liu et al. Tracking vital signs during sleep leveraging off-the-shelf wifi. In *Proceedings of the 16th ACM International Symposium on Mobile Ad Hoc Networking and Computing*, pages 267–276. ACM, 2015.
- [9] X. Liu et al. Wi-sleep: Contactless sleep monitoring via wifi signals. In *Real-Time Systems Symposium (RTSS)*, pages 346–355. IEEE, 2014.
- [10] S. Mallat. *A wavelet tour of signal processing: the sparse way*. Academic press, 2008.
- [11] J. Mäntyjärvi et al. Recognizing human motion with multiple acceleration sensors. In *Systems, Man, and Cybernetics*, volume 2, pages 747–752. IEEE, 2001.
- [12] J. Mäntyjärvi et al. Identifying users of portable devices by gait pattern with accelerometers. In *Acoustics, Speech, and Signal Processing (ICASSP)*, volume 2, pages ii–973. IEEE, 2005.
- [13] G. Molenberghs et al. Review of iris recognition: cameras, systems, and their applications. *Sensor review*, 26(1):66–69, 2006.
- [14] E. Munguia Tapia. *Using machine learning for real-time activity recognition and estimation of energy expenditure*. PhD thesis, Massachusetts Institute of Technology, 2008.
- [15] M. S. Nixon et al. *Human identification based on gait*, volume 4. Springer Science & Business Media, 2010.
- [16] I. Orović et al. A new approach for classification of human gait based on time-frequency feature representations. *Signal Processing*, 91(6):1448–1456, 2011.
- [17] T. C. Pataky et al. Gait recognition: highly unique dynamic plantar pressure patterns among 104 individuals. *Journal of The Royal Society Interface*, 9(69):790–800, 2012.
- [18] M. Robnik-Sikonja and I. Kononenko. Theoretical and empirical analysis of relief and rrelieff. *Machine learning*, 53(1-2):23–69, 2003.
- [19] L. Sun et al. Widraw: Enabling hands-free drawing in the air on commodity wifi devices. In *Proceedings of the 21st Annual International Conference on Mobile Computing and Networking*, pages 77–89. ACM, 2015.
- [20] C. Torrence and G. P. Compo. A practical guide to wavelet analysis. *Bulletin of the American Meteorological society*, 79(1):61–78, 1998.
- [21] P. van Dorp and F. Groen. Feature-based human motion parameter estimation with radar. *Radar, Sonar & Navigation, IET*, 2(2):135–145, 2008.
- [22] C. Wang et al. Human identification using temporal information preserving gait template. *IEEE Transactions on Pattern Analysis and Machine Intelligence*, 34(11):2164–2176, 2012.
- [23] L. Wang et al. Silhouette analysis-based gait recognition for human identification. *IEEE Transactions on Pattern Analysis and Machine Intelligence*, 25(12):1505–1518, 2003.
- [24] W. Wang et al. Understanding and modeling of wifi signal based human activity recognition. In *Proceedings of the 21st Annual International Conference on Mobile Computing and Networking*, pages 65–76. ACM, 2015.
- [25] B. Wei et al. Radio-based device-free activity recognition with radio frequency interference. In *International Conference on Information Processing in Sensor Networks*, pages 154–165. ACM, 2015.
- [26] P. D. Welch. The use of fast fourier transform for the estimation of power spectra: A method based on time averaging over short, modified periodograms. *IEEE Transactions on audio and electroacoustics*, 15(2):70–73, 1967.
- [27] J. Wright et al. Robust face recognition via sparse representation. *IEEE Transactions on Pattern Analysis and Machine Intelligence*, 31(2):210–227, Feb 2009.
- [28] Z. Yang et al. From rssi to csi: Indoor localization via channel response. *ACM Computing Surveys (CSUR)*, 46(2):25, 2013.
- [29] Y. Zeng et al. Analyzing shoppers behavior through wifi signals. In *Proceedings of the 2nd workshop on Workshop on Physical Analytics*, pages 13–18. ACM, 2015.
- [30] Z. Zhou et al. A new human identification method: Sclera recognition. *IEEE Transactions on Systems, Man and Cybernetics, Part A: Systems and Humans*, 42(3):571–583, 2012.